The Astrophysical Journal, 590:999–1007, 2003 June 20

EDDINGTON-LIMITED X-RAY BURSTS AS DISTANCE INDICATORS. I. SYSTEMATIC TRENDS AND SPHERICAL SYMMETRY IN BURSTS FROM 4U 1728−34

Duncan K. Galloway,[1] Dimitrios Psaltis,[1,2] Deepto Chakrabarty,[1,3,4] and Michael P. Muno[1,3]
Received 2002 August 27; accepted 2003 February 28

ABSTRACT

We investigate the limitations of thermonuclear X-ray bursts as a distance indicator for the weakly magnetized accreting neutron star 4U 1728−34. We measured the unabsorbed peak flux of 81 bursts in public data from the *Rossi X-Ray Timing Explorer* (*RXTE*). The distribution of peak fluxes was bimodal: 66 bursts exhibited photospheric radius expansion (presumably reaching the local Eddington limit) and were distributed about a mean bolometric flux of 9.2×10^{-8} ergs cm^{-2} s^{-1}, while the remaining (non–radius expansion) bursts reached 4.5×10^{-8} ergs cm^{-2} s^{-1}, on average. The peak fluxes of the radius expansion bursts were not constant, exhibiting a standard deviation of 9.4% and a total variation of 46%. These bursts showed significant correlations between their peak flux and the X-ray colors of the persistent emission immediately prior to the burst. We also found evidence for quasi-periodic variation of the peak fluxes of radius expansion bursts, with a timescale of $\simeq$40 days. The persistent flux observed with *RXTE*/ASM over 5.8 yr exhibited quasi-periodic variability on a similar timescale. We suggest that these variations may have a common origin in reflection from a warped accretion disk. Once the systematic variation of the peak burst fluxes is subtracted, the residual scatter is only $\simeq$3%, roughly consistent with the measurement uncertainties. The narrowness of this distribution strongly suggests that (1) the radiation from the neutron star atmosphere during radius expansion episodes is nearly spherically symmetric and (2) the radius expansion bursts reach a common peak flux that may be interpreted as a standard candle intensity. Adopting the minimum peak flux for the radius expansion bursts as the Eddington flux limit, we derive a distance for the source of 4.4–4.8 kpc (assuming $R_{\rm NS} = 10$ km), with the uncertainty arising from the probable range of the neutron star mass $M_{\rm NS} = 1.4$–$2\ M_\odot$.

Subject headings: equation of state — nuclear reactions, nucleosynthesis, abundances — stars: individual (4U 1728−34) — stars: neutron — X-rays: bursts — X-rays: individual (4U 1728−34)

1. INTRODUCTION

Thermonuclear (type I) X-ray bursts manifest as rapid changes in the X-ray intensity of accreting neutron stars in low-mass X-ray binary (LMXB) systems, with rise times between $\lesssim$1 and 10 s and decay times between $\sim$10 and 100 s (for reviews, see Lewin, van Paradijs, & Taam 1993; Bildsten 1998). Such bursts have been observed from more than 70 sources (Liu, van Paradijs, & van den Heuvel 2001) and are caused by the unstable nuclear burning of accreted matter on the neutron star surface.

If the thermonuclear energy during a burst is released sufficiently rapidly, the flux through the neutron star atmosphere may reach the local Eddington limit, at which point the outward radiation force balances gravity. The excess energy is converted into potential and kinetic energy of the X-ray photosphere, which is lifted above the neutron star surface while the emerging luminosity (measured locally) remains approximately constant and equal to the Eddington limit. These are the so-called radius expansion or Eddington-limited bursts.

For spherically symmetric emission, the Eddington luminosity measured by an observer at infinity is given by (Lewin et al. 1993)

$$L_{\rm Edd,\infty} = \frac{8\pi G m_p M_{\rm NS} c[1 + (\alpha_T T_{\rm eff})^{0.86}]}{\xi \sigma_{T_{\rm eff}}(1+X)} \left(1 - \frac{2GM_{\rm NS}}{Rc^2}\right)^{1/2}$$
$$= 2.5 \times 10^{38} \left(\frac{M_{\rm NS}}{M_\odot}\right) \frac{1 + (\alpha_{\rm T} T_{\rm eff})^{0.86}}{\xi(1+X)} \times \left(1 - \frac{2GM_{\rm NS}}{Rc^2}\right)^{1/2} \text{ ergs s}^{-1}\ , \quad (1)$$

where $M_{\rm NS}$ is the mass of the neutron star, $T_{\rm eff}$ is the effective temperature of the atmosphere, α_T is a coefficient parameterizing the temperature dependence of the electron scattering opacity (Lewin et al. 1993; $\simeq 2.2 \times 10^{-9}$ K^{-1}), X is the mass fraction of hydrogen in the atmosphere ($\approx$0.7 for cosmic abundances), and the parameter ξ accounts for the possible anisotropy of the burst emission. The final factor in parentheses represents the gravitational redshift due to the compact nature of the neutron star, and it also depends on the height of the emission above the neutron star surface, $R \geq R_{\rm NS}$. Because the Eddington luminosity depends on the ratio $M_{\rm NS}/R_{\rm NS}$, measurements of the peak flux of radius expansion bursts allow, in principle, the measurement of these fundamental properties (e.g., Damen et al. 1990; Smale 2001; Kuulkers et al. 2002). On the other hand, because the masses and radii of stable neutron stars predicted by any given equation of state span a narrow range of

[1] Center for Space Research, Massachusetts Institute of Technology, Cambridge, MA 02139; duncan@space.mit.edu, deepto@space.mit.edu, muno@space.mit.edu.
[2] Current address: School of Natural Sciences, Institute for Advanced Study, Einstein Drive, Princeton, NJ 08540; dpsaltis@ias.edu.
[3] Department of Physics, Massachusetts Institute of Technology.
[4] Alfred P. Sloan Research Fellow.

values (see, e.g., Lattimer & Prakash 2001), Eddington-limited X-ray bursts can be used as distance indicators.

The validity of the physical picture of Eddington-limited bursts discussed above can be verified observationally in two ways. First, the peak fluxes of such bursts from each individual source should be the same. Second, the peak luminosities inferred for sources with independent distance measurements, such as those in globular clusters, should correspond to the Eddington limit for a neutron star. Since the original discovery of Eddington-limited bursts, a number of authors have addressed these questions. In early observations, a significant number of radius expansion bursts had been detected from three sources, and their peak fluxes were found to be similar to within $\simeq$20% (4U 1820−30: Vacca, Lewin, & van Paradijs 1986; Damen et al. 1990; 4U 1636−536: Damen et al. 1990; 4U 1728−34: Basinska et al. 1984). In particular, the peak luminosities of radius expansion bursts observed from 4U 1820−30, which resides in the globular cluster NGC 6624, were found to be comparable to the Eddington limit for a neutron star. Although successful in providing support to the model of Eddington-limited bursts, these early studies were limited to a small number of sources and suffered from the statistical uncertainties inherent to fitting spectral models to low signal-to-noise data. In recent years, observations with *BeppoSAX* and the *Rossi X-Ray Timing Explorer* (*RXTE*) have revealed a large number of Eddington-limited bursts from several sources, which have been studied in great detail. Using *BeppoSAX* and *RXTE* data, Kuulkers et al. (2003) recently studied the Eddington-limited bursts of 12 globular cluster sources with well-known distances and showed that, with one exception, their peak fluxes were constant to within $\simeq$15% and were comparable to the Eddington limit for neutron stars with hydrogen-poor atmospheres.

In this series of articles, we use all the publicly available data obtained with *RXTE* to date in order to observationally test the hypothesis that Eddington-limited bursts can be used as distance indicators for neutron star LMXBs. In the present study we quantify, and examine the causes of, systematic variations in the peak burst flux from the source with the greatest number of bursts detected by *RXTE*, 4U 1728−34.

2. *RXTE* OBSERVATIONS OF 4U 1728−34

The X-ray source 4U 1728−34 (GX 354+0; $l = 354.^\circ3$, $b = -0.^\circ15$) was first resolved by *Uhuru* scans of the Galactic center region (Forman, Tananbaum, & Jones 1976). Thermonuclear X-ray bursts from 4U 1728−34 were discovered during *SAS 3* observations (Lewin, Clark, & Doty 1976; Hoffman et al. 1976). The bursting behavior was subsequently studied in detail using extensive observations by *SAS 3*, which accumulated 96 bursts in total. From these data Basinska et al. (1984) showed evidence for a narrow distribution of peak burst fluxes, as well as a correlation between the peak flux and the burst fluence. The distance to the source has previously been estimated from measurements of the peak burst fluxes as between 4.2 and 6.4 kpc (van Paradijs 1978; Basinska et al. 1984; Kaminker et al. 1989). The estimated extinction to the source is $A_V \approx 14$; only a precise position following from the detection of a radio counterpart allowed identification with a $K = 15$ infrared source (Martí et al. 1998). No independent distance measurement is available. Long-term *Ariel 5* measurements, as well as the first 2 yr of monitoring by the all-sky monitor (ASM) on board *RXTE*, suggest the presence of a long-term quasi periodicity of 63 or 72 days, respectively (Kong, Charles, & Kuulkers 1998).

RXTE/Proportional Counter Array (PCA) observations of the source in 1996 led to the discovery of nearly coherent millisecond oscillations during the X-ray bursts (Strohmayer et al. 1996). Similar oscillations were subsequently observed in nine other sources (van der Klis 2000; Wijnands, Strohmayer, & Franco 2001; Galloway et al. 2001; Kaaret et al. 2002). A substantial archive (1140 ks) of public *RXTE*/PCA data from 4U 1728−34 has accumulated throughout these observations, dating from shortly after the launch of the satellite on 1995 December 30. Subsets of the bursts observed during the PCA observations have been studied by van Straaten et al. (2001) and Franco (2001), with particular attention given to the relationship between the appearance of burst oscillations and the mass accretion rate. A significant fraction of the bursts observed by *RXTE* show evidence for photospheric radius expansion, exhibiting the characteristic temporary increase in the apparent blackbody radius, coincident with a decrease in the color temperature in the early stages of the burst. Muno et al. (2001) used this data set to find a correlation between the frequency of the burst oscillations and the preferential appearance in radius expansion or non–radius expansion bursts in nine sources.

We have obtained all the available public *RXTE* data to date from the High-Energy Astrophysics Science Archive Research Center (HEASARC).[5] This study is part of a larger effort involving more than 70 known bursters; the burst detection and analysis procedures, as well as the resulting burst database, are described in more detail in D. K. Galloway et al. (2003, in preparation). Several of the bursts from 4U 1728−34 we analyzed have also been studied in detail by Strohmayer et al. (1996, 1998; Strohmayer, Zhang, & Swank 1997).

2.1. *All-Sky Monitor*

The ASM on board *RXTE* consists of three scanning shadow cameras (SSCs) sensitive to photons in the energy range 2–10 keV, mounted on a rotating platform (Levine et al. 1996). ASM observations are performed as sequences of dwells lasting 90 s, after which the platform holding the SSCs is rotated by 6°. Most of the sky is viewed once every few hours. The data from each SSC from each dwell are averaged to obtain the daily intensities of known sources in the field of view. The long-term 2–10 keV *RXTE*/ASM flux history of the source is shown in Figure 1. The observed photon flux exhibited variations of $\sim$5 counts s^{-1} on timescales of $\sim$10 days, superposed on a long-term trend of decreasing mean intensity.

We computed the Lomb-normalized periodogram (Press & Rybicki 1989) of the full data set, shown also in Figure 1. We found significant evidence for a periodicity with $P_{\rm ASM} = 38.6$ days, with a Lomb-normalized power of 31.9 as well as secondary peaks at 63.7 and 67.5 days. The latter values are close to those found from earlier *Ariel 5* measurements, as well as a 2 yr subset of the *RXTE*/ASM data by

[5] Additional information on HEASARC is available at http://heasarc.gsfc.nasa.gov.

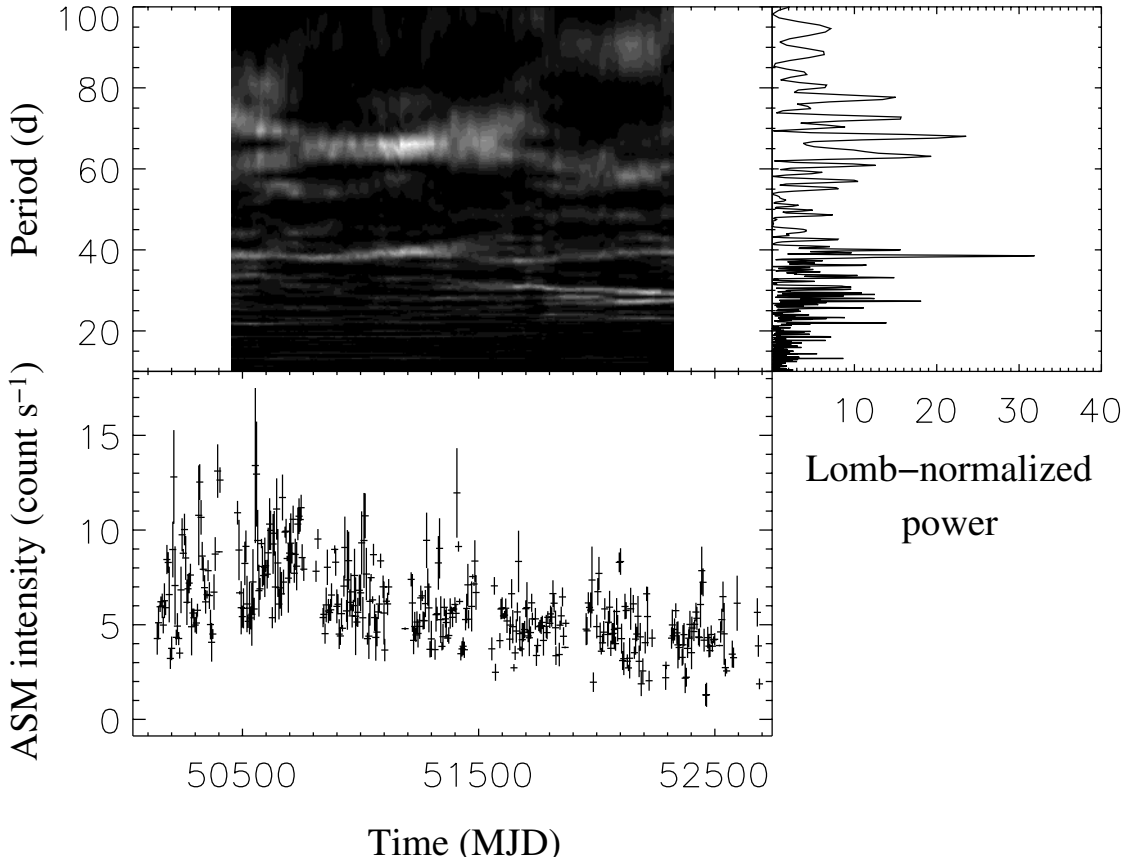

FIG. 1.—Shows *RXTE*/ASM measurements of 4U 1728−34. The top right panel shows the Lomb-normalized periodogram computed over the entire ASM history. The top left panel shows the corresponding dynamical Lomb periodogram, calculated from 730 day subsets of the ASM data at 9 day intervals. The bottom panel shows the 5 day averaged count rates, computed from the initial 1 day averages excluding those points where the measured error is greater than 0.5 counts s^{-1}. Error bars, where shown, indicate the 1 σ uncertainties.

Kong et al. (1998). The rms amplitude of the signal at $P_{\rm ASM}$ was $\simeq$8%–9%. The dynamical Lomb-normalized periodogram shows that this periodicity varied in strength over the entire ASM history (Fig. 1). The $\approx$39 day periodicity appeared strongly only in the first half of the measurement interval, when the source reached its peak long-term intensity. After MJD 51,400, the dominant periodicity appeared to shift to around 30 days. A broad peak around 65 days was also present at most times.

2.2. *Proportional Counter Array*

The PCA (Jahoda et al. 1996) consists of five identical gas-filled proportional counter units (PCUs) with a total effective area of $\approx$6000 cm^2 and sensitivity to X-ray photons in the 2–60 keV range. We initially scanned 1 s binned light curves over the full PCA energy range (created from "Standard-1" mode data) in order to locate X-ray bursts from 4U 1728−34. In all the PCA observations, data were also collected in user-defined modes offering higher time resolution, compared with the standard data modes. The PCA records the arrival time (1 μs resolution) and energy (256 channel resolution) of every unrejected photon; data were generally binned on somewhat lower time and spectral resolution in order to meet telemetry limits. Once an X-ray burst was detected, we extracted 2–60 keV PCA spectra within intervals of 0.25–1 s covering the burst. A response matrix was generated separately for each burst using PCARSP version 8.0 (part of the LHEASOFT release ver. 5.2, 2002 June 25) in order to take into account the known gain variations over the life of the instrument. The gain was manually reset by the instrument team on three occasions (1996 March 21, 1996 April 15, and 1999 March 22); an additional, fifth, gain epoch began on 2000 May 13 with the loss of the propane layer in PCU 0. In addition to these abrupt changes, a more gradual variation in the instrumental response is known to occur because of a number of factors.

We then analyzed these data using an approach that is often used in X-ray burst analysis (e.g., Kuulkers et al. 2002; although see also van Paradijs & Lewin 1986). For the background to the burst spectra we used a spectrum extracted from a (typically) 16 s interval prior to the burst. Each time-resolved background-subtracted spectrum during the bursts was fitted with a blackbody model multiplied by a low-energy cutoff representing interstellar absorption with fixed abundances. The initial spectral fitting was performed with the absorption column density $n_{\rm H}$ free to vary; the resulting fit values typically exhibited very large scatter, particularly toward the end of the burst when the flux was low. Thus, for the final analysis we refitted each spectra with $n_{\rm H}$ fixed at the weighted mean value measured over the entire burst. The unabsorbed bolometric flux $F_{{\rm bol},i}$ at each time step t_i was then estimated according to

$$F_{{\rm bol},i} = \sigma T_i^4 \left(\frac{R_{\rm NS}}{d}\right)_i^2 = 1.0763 \times 10^{-11}\ T_{{\rm bb},i}^4 K_{{\rm bb},i}^2 \ {\rm ergs\ cm^{-2}\ s^{-1}}\ , \quad (2)$$

where R_{NS} is the neutron star radius, d is the distance to the source, T_{bb} is the blackbody (color) temperature in units of keV, and K_{bb} is the normalization of the blackbody component as returned by the fitting program (XSPEC, ver. 11). We also estimated the burst fluence E_b by integrating the measured $F_{bol,i}$ over the burst duration. We discuss the possible consequences of the bolometric correction implicit in equation (2) in § 3.1. Kuulkers et al. (2002) and other authors have noted a ≈20% systematic flux offset in *RXTE* measurements compared with other instruments. It may be argued that the absolute flux calibration of these instruments is no better than that of *RXTE*; in any case, the *RXTE* data still offer substantially better signal-to-noise ratios and hence greater precision of flux measurements. Throughout this paper we quote the unadjusted *RXTE* peak fluxes, but for distance estimates (see § 3.4) we consider the possible effects of this systematic offset.

To measure the (preburst) persistent flux we estimated the instrumental background using PCABACKEST version 3.0 and fitted the background-subtracted preburst spectrum with an absorbed blackbody and power-law model. The typical reduced χ^2 (χ^2_ν) was 1.2. Gain-corrected X-ray colors were also calculated from the preburst spectrum. We determined correction factors for the count rates in the various energy bands by comparison of Crab spectra over the lifetime of the instrument (see Muno, Remillard, & Chakrabarty 2002b for more details of the correction method). The soft color was calculated as the ratio between the background-subtracted gain-corrected count rates in the 3.6–5.0 and 2.2–3.6 keV bands, and the hard color was calculated as the ratio between counts in the 8.6–18 and 5.0–8.6 keV bands.

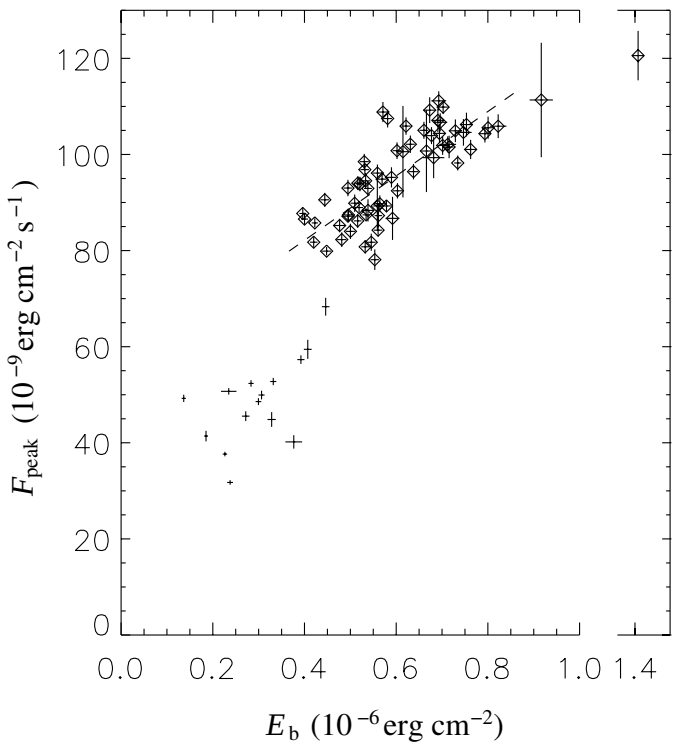

FIG. 2.—Peak flux F_{peak} (excluding the preburst persistent emission) plotted as a function of the integrated burst fluence E_b of 15 non–radius expansion (*cross*) and 66 radius expansion (*diamonds*) bursts from 4U 1728−34. The result of a linear fit to F_{peak} as a function of E_b for the radius expansion bursts is plotted as a dashed line. Error bars indicate the 1 σ uncertainties. Note the broken x-axis.

2.3. *Peak Burst Fluxes*

We detected 81 X-ray bursts observed by *RXTE* from 4U 1728−34 between 1996 February 15 and 2001 November 15, with peak burst fluxes in the range $(0.3–1.2) \times 10^{-7}$ ergs cm^{-2} s^{-1}. We also detected four much fainter bursts, which peaked at $\approx 5 \times 10^{-9}$ ergs cm^{-2} s^{-1}: two on 1996 May 3, and one each on 2001 May 27 and May 29. These burst times closely followed active periods of the nearby source MXB 1730−33 (the "Rapid Burster"), just 0°.53 away, compared with the field of view of *RXTE* of 1°. Since the next brightest burst from 4U 1728−34 was a factor of 6 brighter, we conclude that the four very faint bursts actually originated with the Rapid Burster and exclude them from our analysis.

Most of the X-ray bursts from 4U 1728−34 exhibited some degree of radius expansion. As a working definition, we considered that the local Eddington limit had been reached when (1) the blackbody normalization K_{bb}, which is directly related to the surface area of the emitting region, reached a local maximum close to the time of peak flux; (2) lower values of the normalization K_{bb} were measured following the maximum, with the decrease significant to 4 σ or more; and (3) there was evidence of a significant (local) decrease in the fitted temperature T_{bb} at the same time as the increase in the normalization K_{bb}. For eight of the bursts there was weak evidence of radius expansion, at only the 2–3 σ level. However, the distribution of peak fluxes in this class of bursts was consistent with that of the bursts exhibiting more significant radius expansion, and so we treated them as one population.

The peak bolometric fluxes $F_{peak} = \max(F_{bol,i})$ were bimodally distributed, with the radius expansion bursts around a mean of 9.2×10^{-8} ergs cm^{-2} s^{-1} and the non–radius expansion bursts around a mean of 4.5×10^{-8} ergs cm^{-2} s^{-1} (Fig. 2). The peak fluxes of the radius expansion bursts were roughly proportional to the fluence, up to an asymptotic level of $\approx 1.2 \times 10^{-7}$ ergs cm^{-2} s^{-1} (Spearman's rank correlation $\rho = 0.78$, significant at approximately the 6 σ confidence level). The burst fluence generally ranged $(0.04–0.9) \times 10^{-6}$ ergs cm^{-2}. The non–radius expansion bursts had fluences below 0.5×10^{-6} ergs cm^{-2}, while the majority of the radius expansion bursts had fluences $(0.4–0.8) \times 10^{-6}$ ergs cm^{-2}. The brightest radius expansion burst (72 on 2001 February 9 at 03:01.40 UT) also had the largest fluence. While its peak flux at $(1.21 \pm 0.05) \times 10^{-7}$ ergs cm^{-2} s^{-1} was around 30% larger than the mean for the remaining radius expansion bursts, the fluence was almost 150% greater than the mean at $(1.409 \pm 0.016) \times 10^{-6}$ ergs cm^{-2}.

In the radius expansion bursts, the peak flux was generally reached during the contraction stage following the radius maximum. This is contrary to basic theory of Eddington-limited bursts, which predicts that the observed bolometric flux should be constant throughout the radius expansion and contraction (once the flux is corrected for the effect of gravitational redshift, which is naturally variable due to the changing elevation of the photosphere above the neutron star surface). Furthermore, as noted by van Straaten et al. (2001), some bursts exhibited unusual variation of the fitted radius as the burst evolved. In about half the bursts the radius expansion and subsequent contraction

were highly significant, but following the radius minimum (which is usually assumed to be the time when the expanding material "touches down" on the neutron star surface) the apparent radius increased again, up to a level that in some cases was as high as the initial radius maximum. Since the initial rise and fall in the fitted radius generally exceeded our criteria for classification as a radius expansion burst, we included these unusual cases with the other "normal" radius expansion bursts. However, there are clearly additional factors influencing the observed spectra throughout the burst (Sugimoto, Ebisuzaki, & Hanawa 1984, possibly involving changes in the photospheric composition, perhaps related to ejection of an hydrogen-rich envelope). While these additional effects may also help to determine the peak flux of radius expansion bursts, in general their greatest influence appears to be on the evolution later in the burst, after the initial 5 s or so when the radius expansion takes place.

2.4. *Peak Flux Variation in Radius Expansion X-Ray Bursts*

The peak fluxes of the radius expansion bursts from 4U 1728−34 show a significant ($\chi^2 = 1760$ for 60 degrees of freedom) deviation from a constant value (Fig. 3). The standard deviation of the peak fluxes was 8.7×10^{-9} ergs cm^{-2} s^{-1}, corresponding to a fractional rms of 9.4%; the net variation was 46%.

While the bursts were clustered extremely irregularly in time (primarily due to the irregular scheduling of pointed observations) the peak fluxes of radius expansion bursts that were close in time gave a strong suggestion of systematic evolution, on timescales of a few tens of days. To illustrate this evolution, we calculated a Lomb-normalized periodogram of the peak flux of the radius expansion bursts. Like the ASM periodicity, the timescale of the variation in the peak fluxes did not appear to be consistent over the full set of bursts we measured from *RXTE* observations. Thus, we selected only those bursts before MJD 51,500 to calculate the periodogram (note that this is also when the ∼40 day periodicity in the ASM light curve became much weaker; see Fig. 1). The periodogram shows evidence for excess power between 30 and 60 days; the most significant peak was at 38 days, with a Lomb power of 16.3 (estimated significance greater than 5 σ from Monte Carlo simulations; see Fig. 4). We fitted the peak fluxes folded on the 38 day period with a sine curve, with a resulting fractional rms amplitude of 7.7%. The next most significant peak in the periodogram was at 26 days, with a Lomb power of 9.0 (3.1 σ). Additional evidence that the changes in the peak burst flux was linked to the long-term source evolution comes from significant correlations measured between $F_{\rm peak,\,RE}$ and both the hard and soft gain-corrected colors (Fig. 5). The (Spearman's) rank correlation between the soft color and $F_{\rm peak,\,RE}$ was $\rho = 0.62$, with a significance of 6.8×10^{-6} (equivalent to 4.5 σ); for the hard color, the correlation was $\rho = 0.84$, with a significance of 3.4×10^{-15} (equivalent to 6.1 σ).

While the 38 day periodicity found in the radius expansion burst peak fluxes was corroborated by a significant detection at a similar period in the ASM flux history, the 26 day period was not. Thus, we consider the evidence for the presence of the latter signal to be weak. The apparent

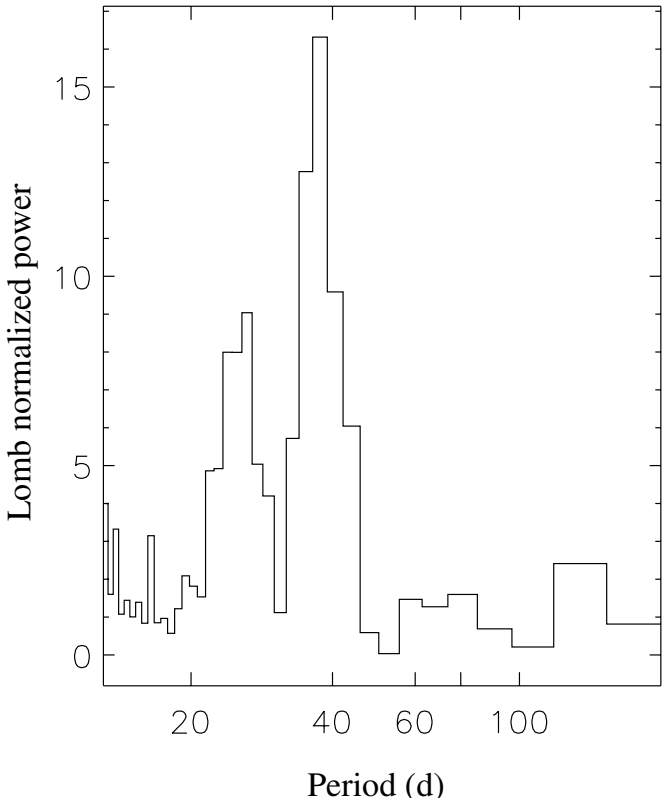

FIG. 4.—Shows the Lomb-normalized periodogram of the time variation of the peak fluxes $F_{\rm peak,\,RE}$ from 50 radius expansion bursts occurring before MJD 51,500 (of 66 radius expansion bursts in total). Note the indications for excess power between 30 and 60 days; the most significant peak is at 38 days, with a Lomb power of 16.3.

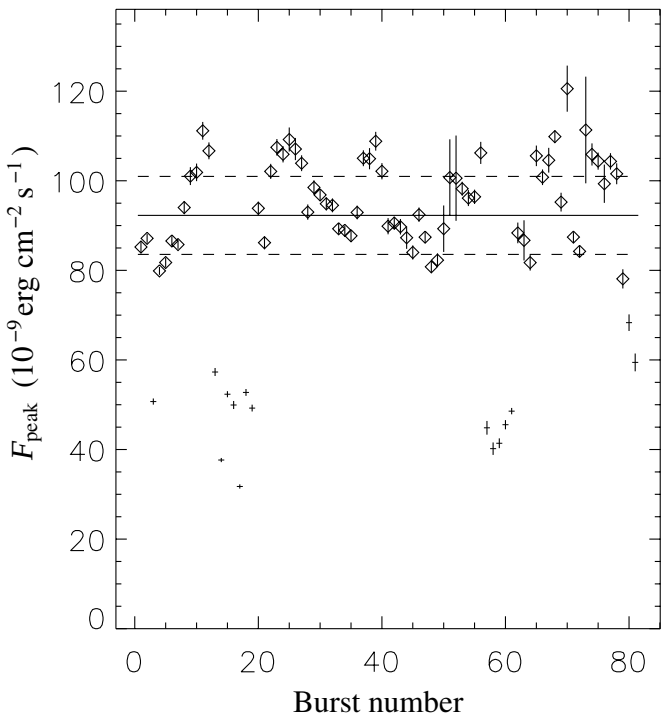

FIG. 3.—Peak fluxes $F_{\rm peak}$ (excluding the preburst persistent emission) of 81 X-ray bursts from 4U 1728−34 as a function of burst number, which increases monotonically with time. The horizontal solid line shows the mean peak flux of the radius expansion bursts (*diamonds*), while the dashed lines show the 1 σ limits. Error bars indicate the 1 σ uncertainties on each measurement.

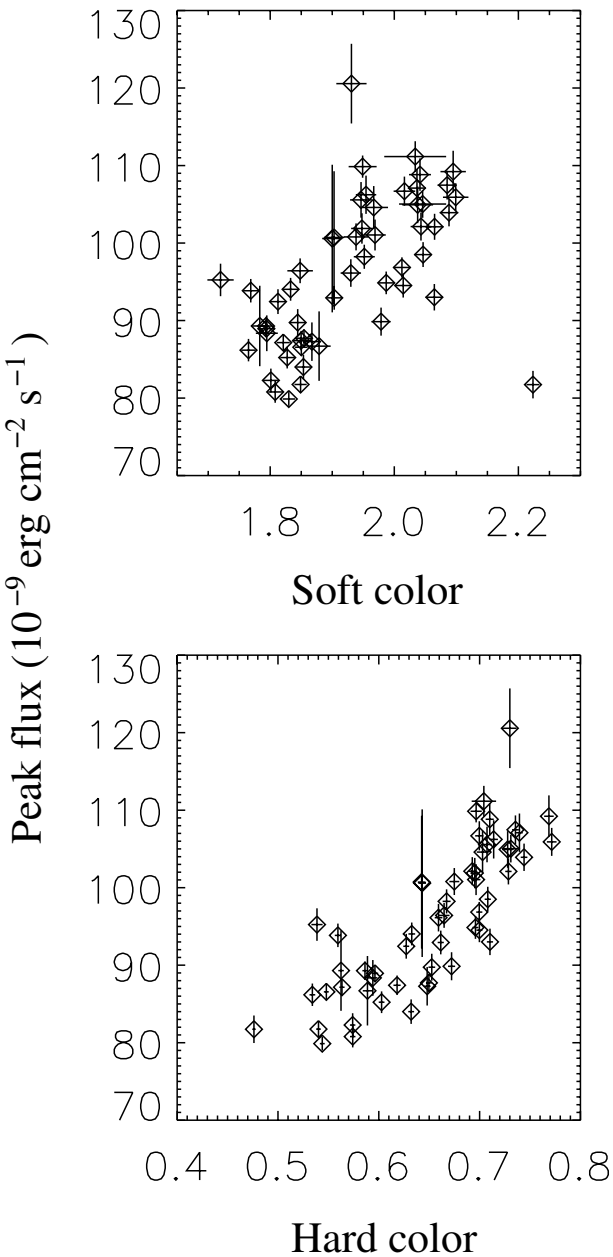

FIG. 5.—Peak flux $F_{\rm peak,RE}$ of radius expansion thermonuclear X-ray bursts from 4U 1728−34, as a function of the gain-corrected soft (3.5–5.0/2.2–3.6 keV) and hard (8.6–18/5.0–8.6 keV) X-ray colors of the persistent flux, prior to each burst. Error bars represent the estimated 1 σ uncertainties.

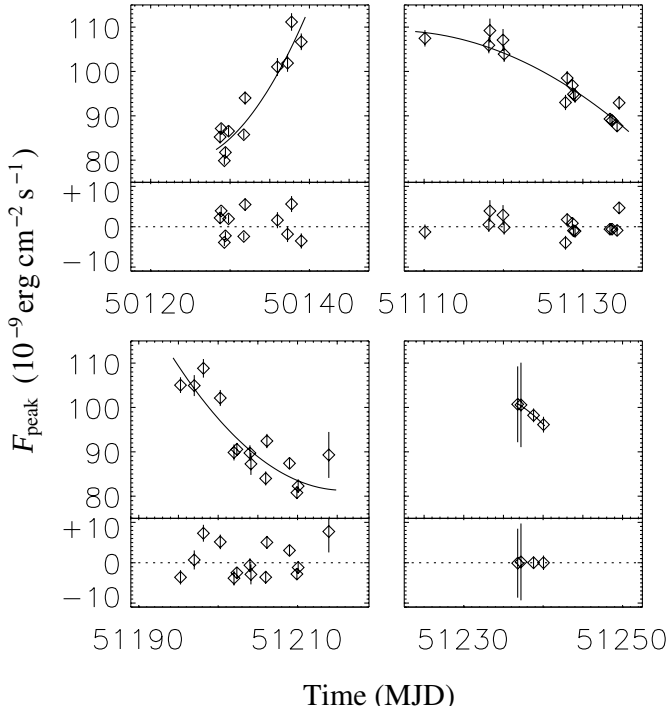

FIG. 6.—Peak burst fluxes $F_{\rm peak,RE}$ of selected subsets of radius expansion bursts from 4U 1728−34, with the best-fit second-order polynomial overplotted as a solid line. The bottom part of each panel shows the residuals after the polynomial fit is subtracted. Error bars show the 1 σ uncertainties.

quasi-periodic behavior of the ASM flux modulation, coupled with the similarity in the timescales and modulation amplitudes of the ASM flux and the radius expansion burst peak fluxes, suggest that these two phenomena share a common cause. The uneven time sampling of $F_{\rm peak,RE}$ and the time dependence of the ASM periodicity (Fig. 1) did not allow us to test this hypothesis for the entire set of radius expansion bursts. However, we have identified four intervals, in which multiple radius expansion bursts were detected over time spans of no more than ≈30 days. The resulting four subsamples contain a total of 41 of the 66 radius expansion bursts measured from 4U 1728−34. For each of these intervals we attempted to remove the long-term variation by fitting the overall $F_{\rm peak,RE}$ time dependence using a second-order polynomial (Fig. 6). The combined distribution of the residuals from each of the polynomial fits is shown in Figure 7. The distribution is consistent with Gaussian noise with $\sigma = 3.2\%$ of the mean peak flux, compared with the averaged 1 σ flux measurement errors of 2.1%.

3. DISCUSSION

We have studied 81 thermonuclear X-ray bursts from 4U 1728−34, which includes 66 exhibiting evidence for photospheric radius expansion, as observed by the *RXTE*/PCA. We have shown that the radius expansion bursts exhibit a significant variation in their peak fluxes $F_{\rm peak,RE}$. The fractional standard deviation was ≃9.4%, while the total variation was ≃46%. This is significantly larger than the formal measurement errors, which were typically ≃2%. This result appears inconsistent with the simple picture of radius expansion bursts (e.g., Lewin et al. 1993), according to which the peak flux should be nearly constant and equal to the Eddington critical flux. However, we must also consider the possibility of a variety of systematic effects arising as a consequence of our analysis method, which may contribute (or give rise) to the measured variation.

3.1. *Possible Systematic Effects*

While subtraction of the preburst emission as background has dubious theoretical justification and may originally have been adopted for convenience, the method has been shown in several analyses to be relatively robust (e.g., van Paradijs & Lewin 1986; Kuulkers et al. 2002). An implicit assumption is that the persistent emission remains

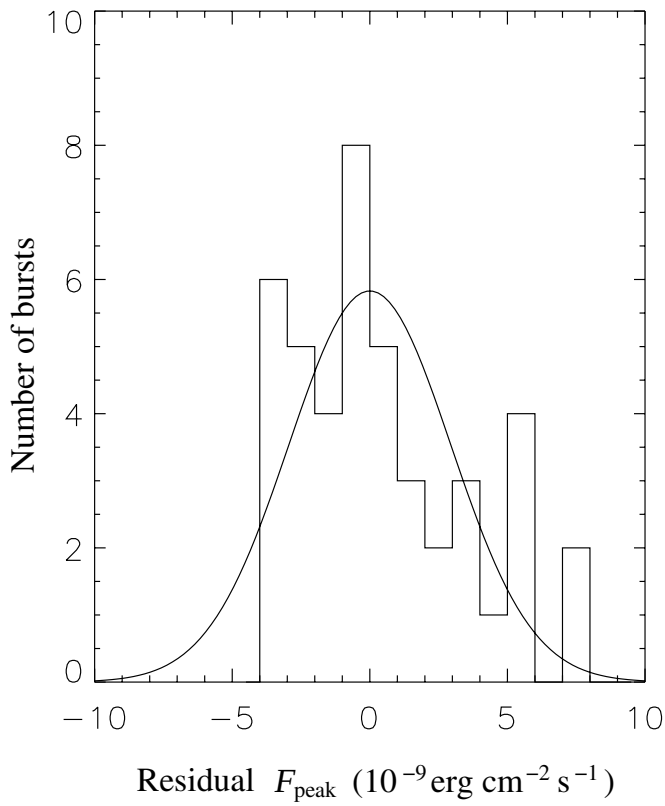

FIG. 7.—Combined distribution of residuals from the fits shown in Fig. 6, with the expected Gaussian distribution for the measured $\sigma = 2.8\%$ overplotted.

unchanged throughout the burst. This may not be true, especially for the very energetic radius expansion bursts that may disrupt the inner accretion flow. As a result, variations in the true persistent flux $F_{\rm per}(t)$ during the burst may contribute to variation in the measured bolometric burst flux. The persistent flux prior to the radius expansion bursts in 4U 1728−34 was typically around 3.7×10^{-9} ergs cm^{-2} s^{-1}, but for some bursts it was as high as 5×10^{-9} ergs cm^{-2} s^{-1}. The net variation over all the bursts was only 3.2×10^{-9} ergs cm^{-2} s^{-1}, which is insufficient to account for the 4.2×10^{-8} ergs cm^{-2} s^{-1} net variation in the peak burst fluxes. Even if the persistent flux were quenched completely during the burst, this would still only give a variation of at most 5×10^{-9} ergs cm^{-2} s^{-1}. Thus, variations in the persistent flux cannot completely account for the observed variation in $F_{\rm peak,RE}$ but may contribute to some extent. If this is the case, we may expect a correlation between the $F_{\rm peak,RE}$ and the preburst persistent flux. In fact, $F_{\rm peak,RE}$ and the persistent flux were weakly anticorrelated, with Spearman's rank correlation $\rho = -0.32$ (estimated significance 1.5×10^{-2}, equivalent to 2.4 σ). If anything, the persistent flux variation serves to slightly suppress the true variation in $F_{\rm peak,RE}$.

The bolometric correction (eq. [2]) typically adds $\simeq$7% to the peak 2.5–20 keV flux of the radius expansion bursts as measured by the PCA. This correction may influence our result in one of two ways. On one hand, systematically biased bolometric corrections may give rise to a variation in flux that is not present in the observed source fluxes (restricted to the PCA passband). We can easily rule out this possibility, since the flux integrated just over the PCA passband exhibits identical (fractional) variation as the inferred bolometric flux. Alternatively, deviations in the spectrum from a perfect blackbody may give rise to (unobserved) variations in the flux outside the PCA passband that contribute to the true bolometric flux variation. In the latter case these unobserved bolometric flux variations may (for example) partially or completely compensate for the variation we see in the PCA passband, so that the bolometric flux variation we infer is exaggerated, or erroneous. The second effect is more difficult to discount, since (obviously) the spectral variations outside the PCA passband are not measurable with the present data. However, the $\simeq$7% typically added to the flux in the PCA passband by the bolometric correction is significantly smaller than the $\simeq$46% observed variation in the peak fluxes. In order to compensate for the flux variation we observe, this contribution would then need to fluctuate by a factor of $\simeq$6, which seems unlikely.

Thus, we conclude that the observed variation was not an artifact of any aspect of our analysis method and hence must be genuine.

3.2. *Origin of the Peak Flux Variation*

The large number of radius expansion bursts observed from 4U 1728−34 with *RXTE*/PCA along with the long-term flux history accumulated by the ASM provides for the first time a plausible cause for the observed broad distribution of peak burst fluxes. The fact that (1) the peak burst fluxes were correlated with the X-ray colors of the persistent emission, (2) they varied in a quasi-periodic manner, and (3) the timescale and fractional amplitude of the variability were similar to those of the persistent emission, strongly suggest that the same phenomenon causes the variability in both the persistent and burst fluxes.

Since the variability of the persistent emission is not coherent, it is unlikely to be due to orbital modulation. As noted by Kong et al. (1998), its timescale (whether $\sim$30 or 60–70 days) is much longer than would normally be expected for the orbital period of a Roche lobe–filling low-mass X-ray binary. Such "superorbital" periodicities are observed in several similar sources (e.g., White, Nagase, & Parmar 1995) and are generally attributed to variations in the accretion geometry, possibly caused by the precession of a warped accretion disk about the neutron star. If the persistent emission is modulated at this timescale because of a slowly evolving warp in the accretion disk that is reflecting a small fraction of the X-ray luminosity of the central object to the observer, then the peak burst fluxes would also be modulated at the same timescale and with a similar amplitude. Our analysis of the radius expansion bursts of 4U 1728−34 strongly suggest that this is the case. Further support is provided by the highly significant correlation observed between the peak flux and the fluence for the radius expansion bursts. If there were no additional contribution to the burst flux from disk reflection, theory predicts that the peak flux would be independent of the fluence.

It remains to be established whether, given the conditions in the 4U 1728−34 system, the accretion disk can become warped, undergo precession at approximately the measured (quasi) periodicities, and give rise to the observed degree of modulation of the persistent and peak radius expansion burst fluxes. For example, the disk warp may arise from

nonaxisymmetric radiation pressure forces (e.g., Pringle 1996; Maloney, Begelman, & Pringle 1996; Maloney & Begelman 1997). The conditions required for the initial warping, and steady precession thereafter, depend primarily on the orbital separation and the efficiency of accretion (Ogilvie & Dubus 2001). The orbital parameters are presently unknown for 4U 1728−34 but are in principle measurable; the accretion efficiency is much more difficult to measure for this or any other LMXB. Thus, our present level of knowledge is not sufficient to reject the hypothesis that a precessing warped disk (whether arising by radiation instabilities or some other mechanism) is present in 4U 1728−34. While the question of whether a disk warp can give rise to the observed modulation is comparatively more straightforward, we are still limited by the lack of measured system parameters, in particular, the inclination. For a flat accretion disk Lapidus & Sunyaev (1985) calculated an anisotropy factor of 2.8, depending on the inclination angle. The precessing of a warped disk is likely to affect the proportion of reprocessed radiation observed during the burst in the same way that varying the inclination would. The derived anisotropy factor is more than sufficient to explain the observed modulation in the peak flux of radius expansion bursts.

Because of these uncertainties, we can most likely adopt a relatively wide range of parameters (e.g., disk warping angle, disk albedo), which will give rise to a modulation of at least the level measured in 4U 1728−34; thus, such an approach would also have no ability to rule out warped disk precession as a mechanism for the X-ray flux modulation. We note that in the archetypical precessing warped disk system Hercules X-1, periodic obscuration of the neutron star by the disk gives rise to a modulation of the persistent X-ray flux of essentially 100% (e.g., Scott, Leahy, & Wilson 2000), much larger than the $\sim$10% measured for 4U 1728−34. Since it exhibits neither X-ray eclipses or dips, 4U 1728−34 must have a lower inclination ($i \lesssim 85°$) than Hercules X-1, making obscuration by the disk less likely. For a disk warped to the degree inferred for Hercules X-1 (20° at the outer edge), the *a priori* probability for obscuration in 4U 1728−34 is $\sim$25%. Even if the inclination is not sufficiently high to permit obscuration, X-ray reflection from the disk, coupled with the variations in the projected disk area due to the precessing warp, may yet be sufficient to give rise to the observed modulation.

3.3. *Possible Anisotropy of the Burst Emission*

When the systematic trends in the variation of the peak burst fluxes are removed, the residual variation is only 2.8%–3.2%, which is comparable to the typical measurement uncertainty of 2%. This has a very important implication for the anisotropy of radius expansion bursts in 4U 1728−34, as described by the parameter ξ in equation (1). The small residual scatter of the peak fluxes strongly suggests that the intrinsic variation of the peak burst flux is also small, $\simeq$1%–2%. It seems unlikely that we observe the same face of the neutron star at the same orientation during every one of these bursts, particularly given the rapid rotation inferred from the burst oscillations (364 Hz; Strohmayer et al. 1996). Additionally, these same oscillations are almost never observed during the radius expansion episode itself, even if they are present earlier or later in the burst (Muno et al. 2002a). We conclude that the longitudinal dependence of the burst flux during the radius expansion episodes is negligible. A latitudinal variation in flux remains plausible, particularly since the effective gravity is smaller at the neutron star equator than at the poles, and so we might expect a greater degree of expansion of the atmosphere there. However, we observe significant variation in the blackbody normalization when the peak burst flux is achieved, which suggests that the radius expansion episodes reach different peak radii. Since we might expect the degree of latitudinal anisotropy to vary with increasing radius, the effect of such a latitudinal variation of flux would be a dependence of the peak flux on the blackbody normalization at the peak, which is not observed. Thus, we conclude that the degree of latitudinal flux anisotropy is most likely also limited by the (inferred) intrinsic variation of the peak burst fluxes. We conclude that the burst emission during the radius expansion episode is isotropic to within $\simeq$1%–2%. Note that it is still possible for the burst emission at the neutron star surface to be significantly anisotropic, but that this anisotropy is smoothed out through reprocessing in the extended atmosphere present during the radius expansion episodes.

3.4. *Consequences for Distance Estimates*

Studies such as this provide a measure of the systematic uncertainties of the distance estimates of X-ray sources that are based solely on Eddington-limited bursts (see, e.g., van Paradijs & White 1995). We note that the standard deviation we measure is within the typical peak burst flux uncertainty ($\simeq$15%) measured by Kuulkers et al. (2003) for the globular cluster burst sources. While the inferred (intrinsic) isotropy of the burst radiation (§ 3.3) allows us to at least eliminate that contribution to uncertainties in distance estimates, the additional systematic error contributed by the observed scatter in the peak burst fluxes is still smaller than the usual other uncertainties due to the unknown neutron star mass and atmospheric composition. Furthermore, without a detailed understanding of the degree of reprocessing occurring in the region around the neutron star, we cannot at this time determine the intrinsic peak luminosity of the radius expansion bursts, from the broad distribution we have observed.

Nevertheless, we now calculate a probable range for the distance to 4U 1728−34, given plausible values for the neutron star mass and atmospheric composition. We identify the minimum peak flux of the radius expansion bursts as the best estimate of the Eddington limit; this burst will have the smallest contribution due to reprocessed radiation and thus will provide the best estimate of the intrinsic maximum flux. Since the peak flux is typically reached near the end of the radius contraction, we calculate the gravitational redshift parameter at the neutron star radius $R_{\rm NS} = 10$ km. We also reduce our observed fluxes by 20% to correct for the observed systematic flux offset measured for *RXTE* (see § 2.2) so that the inferred Eddington flux is 6.2×10^{-8} ergs cm^{-2} s^{-1}. Thus, for a 1.4 (2.0) $M_\odot$ neutron star with cosmic atmospheric abundance ($X = 0.7$), the distance is 4.4 (4.8) kpc. For a pure He atmosphere the distance is 30% greater. These values are roughly consistent with previous estimates (van Paradijs 1978; Basinska et al. 1984; Kaminker et al. 1989) and place the source within 12 pc of the Galactic plane, about 4 kpc from the center.

This research has made use of data obtained through the High Energy Astrophysics Science Archive Research Center (HEASARC) Online Service, provided by the NASA/Goddard Space Flight Center. We thank Mike Nowak, Fred Lamb, and Erik Kuulkers for their helpful comments on the paper. This work was supported in part by the NASA Long Term Space Astrophysics program under grant NAG 5-9184. D. P. acknowledges support from NSF grant PHY-0070928.

REFERENCES

Basinska, E. M., Lewin, W. H. G., Sztajno, M., Cominsky, L. R., & Marshall, F. J. 1984, ApJ, 281, 337
Bildsten, L. 1998, in The Many Faces of Neutron Stars, ed. R. Buccheri, J. van Paradijs, & A. Alpar (Dordrecht: Kluwer), 419
Damen, E., Magnier, E., Lewin, W. H. G., Tan, J., Penninx, W., & van Paradijs, J. 1990, A&A, 237, 103
Forman, W., Tananbaum, H., & Jones, C. 1976, ApJ, 206, L29
Franco, L. M. 2001, ApJ, 554, 340
Galloway, D. K., Chakrabarty, D., Muno, M. P., & Savov, P. 2001, ApJ, 549, L85
Hoffman, J. A., Lewin, W. H. G., Doty, J., Hearn, D. R., Clark, G. W., Jernigan, G., & Li, F. K. 1976, ApJ, 210, L13
Jahoda, K., Swank, J. H., Giles, A. B., Stark, M. J., Strohmayer, T., Zhang, W., & Morgan, E. H. 1996, Proc. SPIE, 2808, 59
Kaaret, P., in 't Zand, J. J. M., Heise, J., & Tomsick, J. A. 2002, ApJ, 575, 1018
Kaminker, A. D., Pavlov, G. G., Shibanov, Y. A., Kurt, V. G., Smirnov, A. S., Shamolin, V. M., Kopaeva, I. F., & Sheffer, E. K. 1989, A&A, 220, 117
Kong, A. K. H., Charles, P. A., & Kuulkers, E. 1998, NewA, 3, 301
Kuulkers, E., den Hartog, P. R., in 't Zand, J. J. M., Verbunt, F. W. M., Harris, W. E., & Cocchi, M. 2003, A&A, 399, 663
Kuulkers, E., Homan, J., van der Klis, M., Lewin, W. H. G., & Méndez, M. 2002, A&A, 382, 947
Lapidus, I. I., & Sunyaev, R. A. 1985, MNRAS, 217, 291
Lattimer, J. M., & Prakash, M. 2001, ApJ, 550, 426
Levine, A. M., Bradt, H., Cui, W., Jernigan, J. G., Morgan, E. H., Remillard, R., Shirey, R. E., & Smith, D. A. 1996, ApJ, 469, L33
Lewin, W. H. G., Clark, G., & Doty, J. 1976, IAU Circ., 2922, 1
Lewin, W. H. G., van Paradijs, J., & Taam, R. E. 1993, Space Sci. Rev., 62, 223
Liu, Q. Z., van Paradijs, J., & van den Heuvel, E. P. J. 2001, A&A, 368, 1021
Maloney, P. R., & Begelman, M. C. 1997, ApJ, 491, L43
Maloney, P. R., Begelman, M. C., & Pringle, J. E. 1996, ApJ, 472, 582
Martí, J., Mirabel, I. F., Rodriguez, L. F., & Chaty, S. 1998, A&A, 332, L45
Muno, M. P., Chakrabarty, D., Galloway, D. K., & Psaltis, D. 2002a, ApJ, 580, 1048
Muno, M. P., Chakrabarty, D., Galloway, D. K., & Savov, P. 2001, ApJ, 553, L157
Muno, M. P., Remillard, R. A., & Chakrabarty, D. 2002b, ApJ, 568, L35
Ogilvie, G. I., & Dubus, G. 2001, MNRAS, 320, 485
Press, W. H., & Rybicki, G. B. 1989, ApJ, 338, 277
Pringle, J. E. 1996, MNRAS, 281, 357
Scott, D. M., Leahy, D. A., & Wilson, R. B. 2000, ApJ, 539, 392
Smale, A. P. 2001, ApJ, 562, 957
Strohmayer, T. E., Zhang, W., & Swank, J. H. 1997, ApJ, 487, L77
Strohmayer, T. E., Zhang, W., Swank, J. H., & Lapidus, I. 1998, ApJ, 503, L147
Strohmayer, T. E., Zhang, W., Swank, J. H., Smale, A., Titarchuk, L., Day, C., & Lee, U. 1996, ApJ, 469, L9
Sugimoto, D., Ebisuzaki, T., & Hanawa, T. 1984, PASJ, 36, 839
Vacca, W. D., Lewin, W. H. G., & van Paradijs, J. 1986, MNRAS, 220, 339
van der Klis, M. 2000, ARA&A, 38, 717
van Paradijs, J. 1978, Nature, 274, 650
van Paradijs, J., & Lewin, W. H. G. 1986, A&A, 157, L10
van Paradijs, J., & White, N. 1995, ApJ, 447, L33
van Straaten, S., van der Klis, M., Kuulkers, E., & Méndez, M. 2001, ApJ, 551, 907
White, N. E., Nagase, F., & Parmar, A. N. 1995, in X-Ray Binaries, ed. W. H. G. Lewin, J. van Paradijs, & E. P. J. van den Heuvel (Cambridge: Cambridge Univ. Press), 1
Wijnands, R., Strohmayer, T., & Franco, L. M. 2001, ApJ, 549, L71